IOP PUBLISHING SEMICONDUCTOR SCIENCE AND TECHNOLOGY

Semicond. Sci. Technol. **24** (2009) 075003 (6pp) doi:10.1088/0268-1242/24/7/075003

Tunneling current via dislocations in Schottky diodes on AlInN/AlN/GaN heterostructures

Engin Arslan[1,2,4], S¸emsettin Altındal[3], Suleyman¨ Ozc¸elik¨[3] and Ekmel Ozbay[1,2]

[1] Nanotechnology Research Center—NANOTAM, Department of Physics, Department of Electrical and Electronics Engineering, Bilkent University, 06800 Ankara, Turkey
[2] Nanotechnology Research Center—NANOTAM, Department of Electrical and Electronics Engineering, Bilkent University, 06800 Ankara, Turkey
[3] Department of Physics, Faculty of Science and Arts, Gazi University, Teknikokullar, 06500 Ankara, Turkey

E-mail: engina@bilkent.edu.tr

Received 24 December 2008, in final form 3 April 2009
Published 26 May 2009
Online at stacks.iop.org/SST/24/075003

Abstract

The forward current–voltage–temperature characteristics of (Ni/Au)–$Al_{0.83}In_{0.17}N$/AlN/GaN heterostructures were studied in a temperature range of 80–375 K. The temperature dependences of the tunneling saturation current (I_t) and tunneling parameters (E_0) were obtained. Weak temperature dependence of the saturation current and the absence of temperature dependence of the tunneling parameters were observed in this temperature range. The results indicate that in the temperature range of 80–375 K, the mechanism of charge transport in the (Ni/Au)–$Al_{0.83}In_{0.17}N$/AlN/GaN heterostructure is performed by tunneling among dislocations intersecting the space-charge region. A model is used for nonuniform tunneling along these dislocations that intersect the space-charge region. The dislocation density that was calculated from the current–voltage characteristics, according to a model of tunneling along the dislocation line, gives the value $7.4 \times 10^8\,cm^{-2}$. This value is close in magnitude to the dislocation density that was obtained from the x-ray diffraction measurements value of $5.9 \times 10^8\,cm^{-2}$. These data show that the current flows manifest a tunneling character, even at room temperature.

(Some figures in this article are in colour only in the electronic version)

1. Introduction

AlGaN/GaNhigh-electronmobilitytransistors(HEMTs)have beenstudiedextensivelyasidealcandidatesforhigh-frequency andhighpowerapplications[1–3]. However, manydifficulties arise from the lattice mismatch and polar surfaces for the commonlyusedAlGaN/GaNheterojunctions[4, 5]. Recently, the AlInN/GaN material system has become of major interest for electronic applications due to its promising electronic properties, polarization effects and high thermal stability [6–8]. An important feature of the $Al_{1-x}In_xN$ alloy is the possibility of growing epitaxial layers that are lattice matched to GaN at an indium content x of approximately 17% [7]. At the lattice-matched $In_{0.17}Al_{0.83}N$/GaN, the heterostructureinterfaceminimizesstrain, therebyminimizing cracking and/or dislocation formation [9, 10]. In addition, at ambient pressure, it allows for the minimization of the piezoelectric polarization that is present in strained systems. However, there is still considerable spontaneous polarization, which is characteristic for nitrides crystallizing in wurtzite structures [9]. Another advantage of using AlInN barriers is their large energy band gap, which together with good mobility properties and low sheet resistance allows for the realization of structures with high electron gas densities, such as high electron mobility transistors [7, 10] and heterojunction field effect transistors [6, 7, 9, 10]. The substantially higher polarization-induced two-dimensional electron gas (2DEG) density, InAlN/GaNHEMTperformanceissuperiorregarding AlGaN/GaN HEMTs [7, 10]. It is for this reason that AlInN materials hold great potential for GaN-based optoelectronics. The performance and reliability of these devices are improved with high-quality Ohmic and Schottky contacts.

The InAlN/GaN HEMT structures are usually grown on highly lattice-mismatched substrates, such as sapphire [4, 5], SiC [11] or Si [12, 13]. Because of the large lattice mismatch and large difference in the thermal expansion coefficients among the GaN film, sapphire and SiC substrate, it is still difficult to obtain a high-quality GaN epilayer [11–13]. This fact causes a high level of in-plane stress and threading dislocation density (DD) generation, as grown by metal-organic chemical vapor deposition (MOCVD) in the GaN epitaxial layer [4, 5, 11–13]. These dislocations affect the performance reliability of the device [3, 4]. If there exist many defects near the surface region, then the electrons can easily go through the barrier by/via defectassisted tunneling, thus greatly enhancing the tunneling probability. It is well established that the crystal quality of Si and GaAs is far superior to that of GaN. For Schottky barriers on Si and GaAs with a doping moderate concentration of $\sim 10^{16}\,cm^{-3}$, tunneling does not play a role in the currenttransport mechanisms. The current-transport mechanisms in devices such as metal–semiconductor (MS), metal–insulator– semiconductor (MIS) and solar cells are dependent on various parameters, such as the process of surface preparation, formation of an insulator layer between the metal and semiconductor, barrier height (BH) inhomogeneity, impurity concentration of a semiconductor, density of interface states or defects, series resistance (R_s) of a device, device temperature and bias voltage. In these devices, different carrier transport mechanisms may dominate the others at a certain temperature and at voltage regions, such as thermionic emission (TE), thermionic-field emission (TFE) and field emission (FE). On the other hand, a simultaneous contribution from two or more mechanisms could also be possible. TFE is important at low temperatures and high doping concentration levels. Recently, experimental results have been shown for MS, MIS and solar cells [14–18]. Among them, Kar *et al* [14] and Cao *et al* [15] presented very interesting studies, where the results indicated the likelihood of a primary currenttransport mechanism to be multistep tunneling and defectassisted tunneling instead of TE, respectively. Evstropov *et al* [16, 17] and Balyaev *et al* [18] showed that the current flow in the III–V heterojunctions is generally governed by multistep tunneling with the involvement of dislocations even at room temperature. They demonstrated that an excess tunnel current canbeattributedtodislocations. Amodeloftunnelingthrough a space-charge region (SCR) along a dislocation line (tube) is suggested [17].

The forward-bias current–voltage (I–V) characteristics at a wide temperature range enable us to understand the different aspects of the current-conduction mechanism and barrier formation. Therefore, the aim of the present study is to investigate the current-transport mechanism in the forward-biased Schottky diode on the InAlN/AlN/GaN heterostructures with a high dislocation compared with the literature in a wide temperature range (80–375 K).

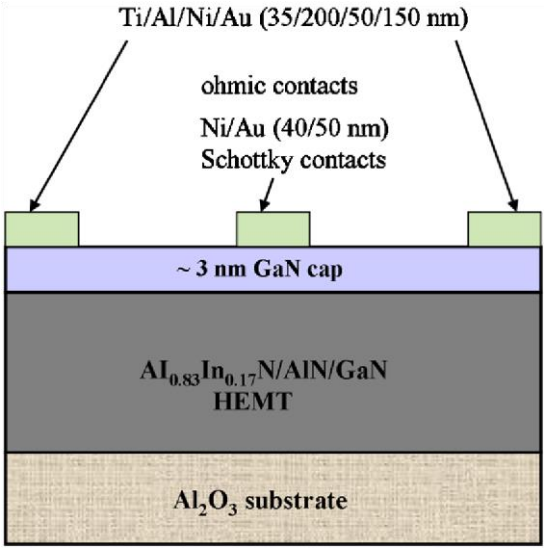

Figure 1. Schematic diagram of the (Ni/Au)–$Al_{0.83}In_{0.17}N$/AlN/GaN heterostructure and view of Ohmic and Schottky contacts on the structures.

2. Experimental procedure

The $Al_{0.83}In_{0.17}N$/AlN/GaN heterostructure on a c-plane

[4] Author to whom any correspondence should be addressed.

0268-1242/09/075003+06$30.00

(0001) Al_2O_3 substrate was grown in a low-pressure MOCVD reactor. Prior to the epitaxial growth, the Al_2O_3 substrate was annealed at 1100 °C for 10 min in order to remove surface contamination. The growth was initiated with a 15 nm thick low-temperature (840 °C) AlN nucleation layer. Then, a 520 nm high-temperature (HT) AlN buffer layer was grown at a temperature of 1150 °C. A 2100 nm thick undoped GaN buffer layer (BL) was then grown at 1070 °C and at a reactor pressure of 200 mbar. Under the GaN BL, a 2 nm thick HT-AlN layer was grown at 1085 °C with a pressure of 50 mbar. Then, an HT-AlN layer was followed by a 20 nm thick AlInN ternary layer. This layer was grown at 800 °C and at a pressure of 50 mbar. Finally, 3 nm thick GaN cap layer growth was carried out at a temperature of 1085 °C and a pressure of 50 mbar.

The Ohmic contacts and Schottky contacts were made atop the surface as square wan de Pauw geometry and 1 mm diameter circular dots, respectively (figure 1). Prior to Ohmic contact formation, the samples were cleaned with acetone in an ultrasonic bath. Then, a sample was treated with boiling isopropyl alcohol for 5 min and rinsed in de-ionized (DI) water. After cleaning, the samples were dipped in a solution of HCl/H_2O (1:2) for 30 s in order to remove the surface oxides and were then again rinsed in DI water for a prolonged period. For the Ohmic contact formation, Ti/Al/Ni/Au (35/200/50/150 nm) metals were thermally evaporated on the sample and were annealed at 850 °C for 30 s in N_2 ambient. After the formation of the Ohmic contact, Ni/Au (40/50 nm) metal evaporation was done as Schottky contacts.

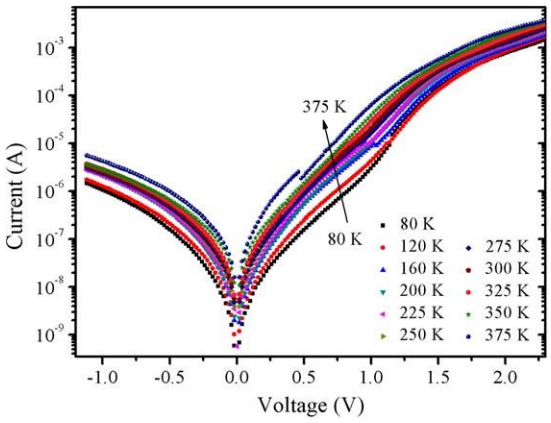

Figure 2. Experimental forward- and reverse-bias semi-logarithmic current–voltage characteristics of the (Ni/Au)–$Al_{0.83}In_{0.17}N$/AlN/GaN heterostructure.

The *I*–*V* measurements were performed by the use of a Keithley 2400 source meter in a temperature range of 80–375 K by using a temperature-controlled Janes vpf-475 cryostat, which enables us to make measurements in the temperature range of 77–450 K. The sample temperature was always monitored by using a copper-constantan thermocouple close to the sample and measured with a Keithley model 199 dmm/scanner and Lake Shore model 321 auto-tuning temperature controllers with sensitivity better than ±0.1 K. The crystalline quality (dislocation density) of the samples was examined by high-resolution x-ray diffraction (HRXRD). The x-ray diffraction was performed by using a Bruker D-8 high-resolution diffractometer system, in turn delivering Cu Kα1 (1.540 A) radiation.˚

3. Results and discussion

Figure 2 shows a set of semi-logarithmic forward-bias *I*–*V* characteristics of an (Ni/Au)–$Al_{0.83}In_{0.17}N$/AlN/GaN heterostructure that was measured in a temperature range of 80–375 K. As can be seen in figure 2, the forward bias of the structure current is an exponential function of the appliedbias voltage in the intermediate voltage regime ($0.1\ V\ V \leqslant 1.4\ V$). It is clear that between the range 10^{-7} and 10^{-4} A of the forward current, the behavior is exponential and beyond that ($I\ \ 10^{-4}$ A) of the plots, thus deviating from this behavior. The deviation at higher current levels is mainly attributed to the series resistance (R_s) of the diode [19]. Moreover, these plots are parallel over a forward-current range of 10^{-7}–10^{-4} A. Also, as seen in figure 2, jumps can be observed in the *I*–*V* profiles at 375 K and ~0.5 V. These jumps can be attributed to the experimental measurements. To interpret the observed electrical characteristics of an (Ni/Au)–$Al_{0.83}In_{0.17}N$/AlN/GaN heterostructure, Riben and Feucht [20] developed a multistep recombination-tunneling model. This model successfully explains the functional dependence of the forward current on the applied voltage and temperature. Themodelassumesthatastaircasepaththatconsistsofaseries of tunneling transitions between trapping levels in the diode space-charge region coupled with a series of vertical steps

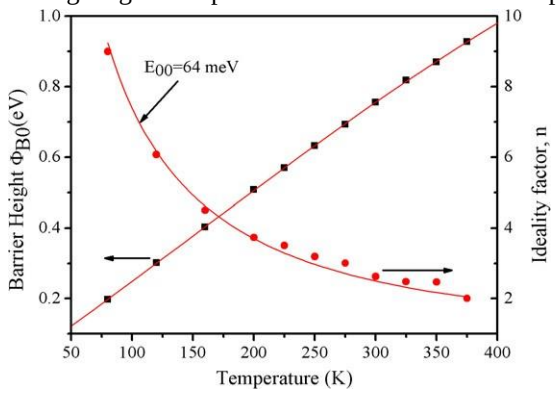

Figure 3. The zero-bias barrier height $_{B0}$ and the ideality factor *n* of the (Ni/Au)–$Al_{0.83}In_{0.17}N$/AlN/GaN heterostructure obtained from the forward-bias *I*–*V* data at various temperatures. The straight line is the least-squares fit of equation (5) to the *n*–*T* data.

where the carrier loses energy by transferring from one level to another. However, such a process is only possible if the concentration of the trapping levels is sufficiently high. In this model, thecarriertunnelingbetweenthedefectlevelsincreases the probability of tunneling through the entire barrier.

The *I*–*V* relation for a Schottky contact based on the thermionic emission theory is given by [21]

$$I = I_0\left(\exp\left(\frac{q(V - IR_s)}{nkT}\right) - 1\right), \tag{1}$$

where I_0 is the saturation current derived from the straight line region of the forward-bias current intercept at a zero bias and is given by

$$I_0 = AA^*T^2\exp\left(-\frac{q\Phi_{B0}}{kT}\right), \tag{2}$$

where A is the contact area, $A*$ is the effective Richardson constant (55.86 A cm^{-2} K^{-2} for undoped $Al_{0.83}In_{0.17}N$) [35], *T* is the absolute temperature in K, *q* is the electron charge, $_{B0}$ is the zero-bias apparent Schottky barrier height, *n* is the ideality factor, *V* is the applied bias voltage and IR_s term is the voltage drop across the series resistance (R_s) of structures.

The ideality factor *n* is calculated from the slope of the linear region of the forward-bias *I*–*V* plot and can be written, from equation (1), as

$$n = \frac{q}{kT}\left(\frac{dV}{d\ln I}\right), \tag{3}$$

where *n* is introduced to take into account the deviation of the experimental *I*–*V* data from the ideal TE theory and should be $n = 1$ for an ideal contact. The experimental values of $_{B0}$ and*n*weredeterminedfromequations(2)and(3), respectively, and are shown in table 1 and figure 3. As seen in table 1 and figure 3, the values of zero-bias barrier height $_{B0}$ and *n* for the (Ni/Au)–$Al_{0.83}In_{0.17}N$/AlN/GaN heterostructure ranged from 0.20 eV and 8.99 (at 80 K) to 0.93 eV and 2.0 (at 375 K),

respectively. Both parameters strongly depend on temperature. While *n* decreases, $_{B0}$ increases with increasing temperature. The values of $_{B0}$ (figure 3) increase with increasing temperature, in which there is a positive coefficient that is in contrast to the negative dependence measurements by

Table 1. Temperature-dependent values of various parameters determined from the forward-bias *I–V* characteristics of the (Ni/Au)–$Al_{0.22}Ga_{0.78}N$/AlN/GaN heterostructure.

		Slope		*nT*	*E*	$\Phi_{B0(I-V)}$
T (K)	I_0 (nA)	(A) (V^{-1})	*n*	(K)	(eV)	(eV)
80	10	16.11	8.99	719.64	0.062	0.20
120	14	15.91	6.07	728.92	0.063	0.30
160	24	16.09	4.50	720.36	0.062	0.40
200	28	15.53	3.73	746.57	0.064	0.51
225	40	14.70	3.50	788.72	0.068	0.57
250	51	14.53	3.19	798.00	0.069	0.63
275	67	14.04	3.00	825.97	0.071	0.69
300	81	14.71	2.63	788.29	0.068	0.75
325	97	14.37	2.48	806.61	0.069	0.82
350	166	13.42	2.47	864.21	0.074	0.87
375	215	15.43	2.00	751.41	0.065	0.93

Crowell and Rideout [22] in silicon Schottky diodes and Mead and Spitzer [23] in InAs and InSb, which closely follows the charge in the forbidden energy bandgap (E_g) with temperature. This contradiction is possible due to equation (2), which is not representative of the reverse saturation current of our samples implying that the current transport is not the TE.

The tunneling current through the barrier is given by [21]

$$I_{\text{tunnel}} = I_t \left\{ \exp\left[\frac{q(V - IR_s)}{E_0} \right] - 1 \right\}, \quad (4)$$

where I_t is the tunneling saturation current and E_0 is the tunneling parameter. E_0 can be defined as [20, 24, 25]

$$E_0 = E_{00} \coth\left(\frac{E_{00}}{kT} \right), \quad (5)$$

where E_{00} is the characteristic tunneling energy that is related to the tunnel effect transmission probability. It is evident that the mechanism of charge transport is a tunnel, which is indicated by the weak temperature dependence of the saturation current. For the tunneling-dominated current transport equation (4), the slope of the ln*I* versus *V* plot ($q/E_0 = q/nkT$) is essentially temperature independent and is called a voltage factor or tunneling constant. In addition, at a constant bias voltage, ln*I* is more of a linear function of temperature than of an inverse temperature. According to the tunneling model, which was developed for Schottky barriers, the band bending works as a barrier for carriers tunneling into interface states or dislocations, where various traps may be involved in multi-tunneling steps [20]. Thermally activated carriers make (step-wise) tunneling into the interface states possible. The values of slope ln*I* versus *V* plots at different temperatures with the corresponding values of the ideality factor (obtained from equation (3)) are shown in table 1 and figure 3. As can be seen in table 1, the *n* values change from 8.99 (at 80 K) to 2.00 (at 375 K). However, the slope and *nT* values remain nearly unchanged over the same temperature range with an average of 15 V^{-1} and 776 K, respectively. The high value of *n* was attributed to several effects such as interface states, tunneling currents in the high dislocations [16–18], image force lowering of the Schottky barrier in the high electric field at an MS interface and generation currents within the space-charge region [21]. The TFE mechanism can

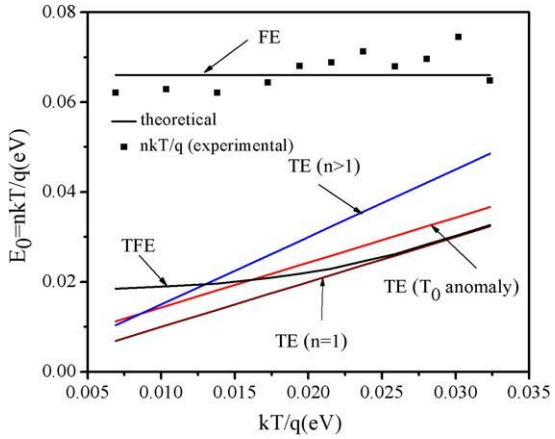

Figure 4. Experimentally and theoretically found tunneling current parameter $E_0(nkT/q)$ versus kT/q for the (Ni/Au)-$Al_{0.83}In_{0.17}N$/AlN/GaN heterostructure.

be ruled out in this region, since *nT* is more or less constant in the measured temperature range. Apart from discussing the main carrier transport mechanisms, the ideality factor is further analyzed by plotting nkT/q against kT/q as shown in figure 4, which shows the experimental and theoretical results of these plots. If FE dominates, then the E_0 data will lie on a straight line as can be seen in figure 4. In this case, E_0 is independent of the temperature and E_0 is very close to the E_{00} values [26]. In our study, the average value of E_0 was found to be 66 meV, which is very close to the 67 meV value of E_{00} that was obtained by fitting equation (5) to the $n(T)$ data (figure 3).

The temperature dependences of I_t and E_0 are shown in figure 5. The results indicate that in the temperature range of 80–375 K, the mechanism of charge transport in the (Ni/Au)–$Al_{0.83}In_{0.17}N$/AlN/GaN heterostructure is tunneling, which is demonstrated by the weak temperature dependence of the saturation current and the absence of the temperature dependence of the tunneling parameters in this temperature range [15–18, 27–30]. The *I–V* behavior of the tunneling current in the barrier structures fabricated based on degenerate semiconductors (Schottky diodes, p–n heterojunctions) can be expressed by equation (4) according to the dislocation model of the tunneling current, in which the tunneling saturation current (I_t) can be represented by the equation of the form [16–18]

$$I_t = qDv_D \exp(-qV_K/E_0), \quad (6)$$

where D is the dislocation density, $v_D \approx 1.5 \times 10^{13}$ s^{-1} is the Debye frequency for the $Al_{0.83}I_{0.17}N$ layer [31] and $qV_K = \Phi_B - \mu_n$ is the diffusion potential for the Schottky barrier diode (SBD). In this equation, $_B$ is the height of the SBD, $\mu_n \cong kT \ln\left(\frac{N_C}{N_D}\right)$ is the chemical potential, N_C is the effective density of states in the conduction band [21], N_D is the concentration of the ionized donors in the AlInN barrier layer and $E_0 = nkT$ is the tunneling parameter.

By using the model equation (6), determining I_t and E_0 from the measured I–V characteristic and knowing $V_K(0)$, the

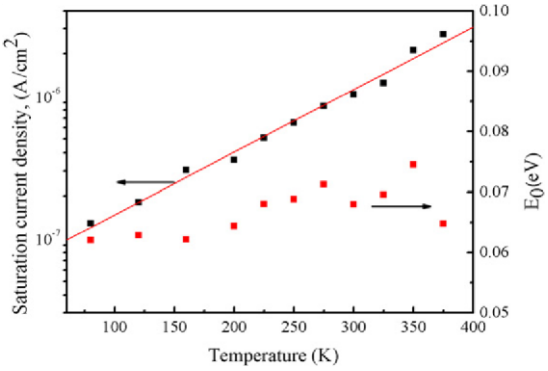

Figure 5. Temperature dependence of the tunneling saturation current I_t and tunneling parameter E_0, which calculated from the tunneling current equation fits to the measured I–V data.

expression for the dislocation density can be expressed as [16–18]

$$D_{dis} = \frac{I}{q\nu} \exp\left[\quad E \quad\right]_{D}^{t(0)} \qquad \frac{qV_K(0)}{0}, \quad (7)$$

where $I_t(0)$ and $E_0(0)$ can be obtained by extrapolation of the absolutetemperatureoftheirtemperaturedependencestozero. The value of $qV_K(0)$ can be calculated from the empirical dependence of $_B$ on the band gap E_g in GaN (because in our study, Schottky diodes were done on GaN cap layers), $\Phi_B \approx \frac{1}{3}E_g^{GaN}$ [18],

$$qV_K(0) = \Phi_B(0) - \mu_n(0) \cong \tfrac{1}{3}E_g^{GaN}(0) - \mu_n(0). \quad (8)$$

The dislocation density can be calculated by equation (7) by using $I_t(0)$, $E_0(0)$, $qV_K(0)$ and $E_g(0) = 3.47$ eV values for GaN. In addition, this case was supported by the experimental values of the height of the Schottky barrier that was formed on the GaN layers by pure metals Ni, Pt, Ir [32] and Au [33].

We calculated the dislocation density for (Ni/Au)–$Al_{0.83}In_{0.17}N$/AlN/GaN heterostructures by using $I_t(0) = 5.31 \times 10^{-8}$ A cm^{-2}, $E_0(0) = 60$ meV and $qV_K(0) = 1.15$ eV values. We obtained the dislocation density for $Al_{0.83}In_{0.17}N$/AlN/GaN heterostructures as 7.4×10^8 cm^{-2}.

The$Al_{0.83}In_{0.17}N$/AlN/GaNheterostructuresweregrown on sapphire with two steps that exhibited high dislocation densities [5, 13, 36]. The dislocation density (DD) of the sample was investigated by the methods of high-resolution diffractometry. There are three main types of dislocations that are present in the GaN epitaxial layers [13, 34, 36]. Theses dislocation densities are the pure edge dislocation with the Burgers vector $\mathbf{b} = \frac{1}{3}\langle 1\,1\,\bar{2}\,0\rangle$ ($\langle a\rangle$), the pure screw dislocation with the Burgers vector $\mathbf{b} = \langle 0\,0\,0\,1\rangle$ ($\langle c\rangle$) and the mixed dislocation with $\mathbf{b} = \frac{1}{3}\langle 11\bar{2}3\rangle$ ($\langle \mathbf{c}+\mathbf{a}\rangle$). The dislocation densities of GaN can be determined from the following equations [34]:

$$D_{screw} = \frac{(0\,0\,2)}{b^2} \quad \beta_2 \qquad = \frac{\beta^2_{(1\,2\,1)}}{9b^2}$$

, D_{edge} (9)

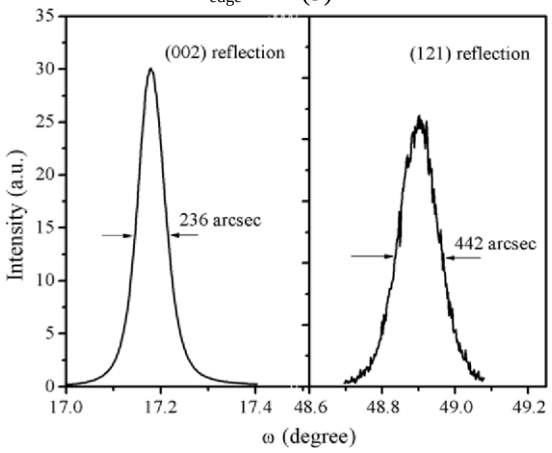

Figure 6. The x-ray rocking curves of the (002) and (121) reflections of the GaN epilayer.

(FWHM) of the measured XRD rocking curves and b is the Burgersvectorlength(b_{screw} =0.5185nm, b_{edge} =0.3189nm). The measured XRD rocking curves for (002) and (121) reflections are shown in figure 6. The FWHM values measured for (002) and (121) reflections are 236 arcsec and 442 arcsec, respectively. By using equations ([1]) and (10), we can calculate the values for the screw, edge and total dislocation densities as 5.4×10^7 cm^{-2}, 5.0×10^8 cm^{-2} and 5.9×10^8 cm^{-2}, respectively. These dislocation density values nearly equal the results that were calculated from those measured from the

where D_{screw} is the screw dislocation density, D_{edge} is the edge dislocation density, β is the full width half-maximum

1 screw edge

$$D_{dis} = D_{screw} + D_{edge}, \quad (10)$$

current-transport measurements. These dislocation densities are consistent with the values given for GaN epitaxial films in the literature [5, 12, 13, 36]. Analysis of the forward-bias *I–V* data indicated that the predominant current mechanism of the $Al_{0.83}In_{0.17}N$/AlN/GaN heterostructure with high dislocation densities in the intermediate-bias voltage region that was investigated in this study was a dislocation-governed currenttransport mechanism rather than other current-transport mechanisms.

4. Conclusion

In conclusion, the temperature-dependent forward-bias current–voltage (*I–V*) characteristics of the (Ni/Au)–$Al_{0.83}In_{0.17}N$/AlN/GaN heterostructure were measured in the temperature range of 80–375 K. The tunneling saturation current (I_t) and tunneling parameter (E_0) were calculated from the *I–V* measurements. The temperature dependence of the tunnel saturation current (I_t) was weak. Moreover, E_0 was nearly independent of the temperature. These results show that the charge transport mechanism in the temperature range of 80–375 K in the forward-biased (Ni/Au)–$Al_{0.83}In_{0.17}N$/AlN/GaN heterostructures was performed by the tunneling mechanism among the dislocations intersecting the space-charge region. The dislocation density (DD) that was calculated from the *I–V* characteristics, according to a model of tunneling along the dislocation line, gives the value 7.4×10^8 cm^{-2}. This value is very close in magnitude to the dislocationdensitythatwasobtainedfromthex-raydiffraction (XRD) measurements value 5.9×10^8 cm^{-2}. These data show that the current flows manifest a tunneling character, even at room temperature.

Acknowledgments

This work is supported by projects EU-NoEMETAMORPHOSE EU-NoE-PHOREMOST and DPT2001-K120590, as well as by Gazi University BAP-05/2006-30 and TUBITAK under project nos. 105E066, 105A005, 106E198 and 106A017. One of the authors (EO) also acknowledges partial support from the Turkish Academy of Sciences.

References

[1] Morkoc¸ H 1999 *Nitride Semiconductors and Devices* (Heidelberg: Springer)
[2] Mohammad S N and Morkoc¸ H 1996 *Prog. Quantum Electron.* **20** 361
[3] Biyikli N, Aytur O, Kimukin I, Tut T and Ozbay E 2002 *Appl. Phys. Lett.* **81** 3272
[4] Arslan E, But¨ un S, Lisesivdin S B, Kasap M, Ozcelik S¨ and Ozbay E 2008 *J. Appl. Phys.* **103** 103701
[5] Yu H, Caliskan D and Ozbay E 2006 *J. Appl. Phys.* **100** 033501
[6] Katz O, Mistele D, Meyler B, Bahir G and Salzman J 2005 *IEEE Trans. Electron Devices* **52** 146
[7] Gonschorek M, Carlin J-F, Feltin E, Py M A and Grandjean N 2006 *Appl. Phys. Lett.* **89** 062106
[8] Gadanecz A, Blasing J, Dadgar A, Hums C and Krost A 2007¨ *Appl. Phys. Lett.* **90** 221906
[9] Katzer D S, Storm D F, Binari S C, Shanabrook B V, Torabi A, Zhou L and Smith D J 2005 *J. Vac. Sci. Technol.* B **23** 1204
[10] Kuzm´ık J, Kostopoulos A, Konstantinidis G, Carlin J-F, Georgakilas A and Pogany D 2006 *IEEE Trans. Electron Devices* **53** 422
[11] Gaska R, Yang J W, Osinsky A, Chen Q, Khan M A, Orlov A O, Snider G L and Shur M S 1998 *Appl. Phys. Lett.* **72** 707
[12] Dadgar A, Hums C, Diez A, Blasing J, Krost A and Cryst J¨ 2006 *Growth* **297** 279
[13] Arslan E, Ozturk M K, Teke A, Ozcelik S and Ozbay E 2008 *J. Phys. D: Appl. Phys.* **41** 155317
[14] Kar S, Panchal K M, Bhattacharya S and Varma S 1982 *IEEE Trans. Electron Devices* **29** 1839
[15] Cao X A, LeBoeuf S F, Kim K H, Sandvik P M, Stokes E B, Ebong A, Walker D, Kretchmer J, Lin J Y and Jiang H X 2002 *Solid-State Electron.* **46** 2291
[16] Evstropov V V, Zhilyaev Yu V, Dzhumaeva M and Nazarov N 1997 *Fiz. Tekh. Poluprovodn.* **31** 152
Evstropov V V, Zhilyaev Yu V, Dzhumaeva M and Nazarov N 1997 *Semiconductors* **31** 115
[17] Evstropov V V, Dzhumaeva M, Zhilyaev Yu V, Nazarov N, Sitnikova A A and Fedorov L M 2000 *Fiz. Tekh. Poluprovodn.* **34** 1357
Evstropov V V, Dzhumaeva M, Zhilyaev Yu V, Nazarov N, Sitnikova A A and Fedorov L M 2000 *Semiconductors* **34** 1305
[18] Belyaev A E, Boltovets N S, Ivanov V N, Kladko V P, Konakova R V, Kudrik Ya Ya, Kuchuk A V, Milenin V V, Sveshnikov Yu N and Sheremet V N 2008 *Semiconductors* **42** 689
[19] Chand S and Bala S 2005 *Semicond. Appl. Surf. Sci.* **252** 358
[20] Riben A R and Feucht D L 1966 *Int. J. Electron.* **20** 583
[21] Sze S M 1981 *Physics of Semiconductor Devices* (New York: Wiley)
[22] Crowell C R and Rideout V L 1969 *Solid-State Electron.* **12** 89
[23] Mead C A and Spitzer W G 1964 *Phys. Rev.* **134** A713 [24] Donoval D, Barus M and Zdimal M 1991 *Solid-State Electron.* **34** 1365
[25] Bayhan H and Sertap Kavasoglu A 2005˘ *Solid-State Electron.* **49** 991
[26] Yu A Y C and Snow E H 1968 *J. Appl. Phys.* **39** 3008
[27] Marchand J J and Truong K 1983 *J. Appl. Phys.* **54** 7034
[28] Ozdemir S and As¸tındal S¸ 1994¨ *Sol. Energy Mater. Sol. Cells* **32** 115
[29] Ashok S, Sharma P P and Fonash S J 1980 *IEEE Trans. Electron Devices* **ED-27** 725
[30] Saxena A N 1969 *Surf. Sci.* **13** 151
[31] Morkoc Hadis 2008 *Handbook of Nitride Semiconductors and Devices: Volume 1: Materials Properties, Physics and Growth* (New York: Wiley-VCH)

[32] Kumar V, Selvanathan D, Kuliev A, Kim S, Flynn J and Adesida I 2003 *Electron. Lett.* **39** 747
[33] Monroy E *et al* 2002 *Semicond. Sci. Technol.* **17** L47
[34] Metzger T *et al* 1998 *Phil. Mag.* A **77** 1013
[35] Levinshtein M, Rumyantsev S L and Shur M S 2001 *Properties of Advanced Semiconductor Materials* (New York: Wiley) [36] Arslan E, Altındal S, Ozc¸elik S and Ozbay E 2009¨ *J. Appl. Phys.* **105** 023705